Published OnlineFirst January 3, 2013; DOI: 10.1158/1078-0432.CCR-12-3072

Clinical Cancer Research

Targeting Activated Akt with GDC-0068, a Novel Selective Akt Inhibitor That Is Efficacious in Multiple Tumor Models

Jie Lin, Deepak Sampath, Michelle A. Nannini, et al.

Clin Cancer Res 2013;19:1760-1772. Published OnlineFirst January 3, 2013.

Published OnlineFirst January 3, 2013; DOI: 10.1158/1078-0432.CCR-12-3072

Cancer Therapy: Preclinical

Clinical Cancer Research

Targeting Activated Akt with GDC-0068, a Novel Selective Akt Inhibitor That Is Efficacious in Multiple Tumor Models

Jie Lin[1], Deepak Sampath[1], Michelle A. Nannini[1], Brian B. Lee[1], Michael Degtyarev[1], Jason Oeh[1], Heidi Savage[1], Zhengyu Guan[1], Rebecca Hong[1], Robert Kassees[1], Leslie B. Lee[1], Tyler Risom[2], Stefan Gross[2], Bianca M. Liederer[1], Hartmut Koeppen[1], Nicholas J. Skelton[1], Jeffrey J. Wallin[1], Marcia Belvin[1], Elizabeth Punnoose[1], Lori S. Friedman[1], and Kui Lin[1]

Abstract

Purpose: We describe the preclinical pharmacology and antitumor activity of GDC-0068, a novel highly selective ATP-competitive pan-Akt inhibitor currently in clinical trials for the treatment of human cancers.

Experimental Design: The effect of GDC-0068 on Akt signaling was characterized using specific biomarkers of the Akt pathway, and response to GDC-0068 was evaluated in human cancer cell lines and xenograft models with various genetic backgrounds, either as a single agent or in combination with chemotherapeutic agents.

Results: GDC-0068 blocked Akt signaling both in cultured human cancer cell lines and in tumor xenograft models as evidenced by dose-dependent decrease in phosphorylation of downstream targets. Inhibition of Akt activity by GDC-0068 resulted in blockade of cell-cycle progression and reduced viability of cancer cell lines. Markers of Akt activation, including high-basal phospho-Akt levels, PTEN loss, and PIK3CA kinase domain mutations, correlate with sensitivity to GDC-0068. Isogenic PTEN knockout also sensitized MCF10A cells to GDC-0068. In multiple tumor xenograft models, oral administration of GDC-0068 resulted in antitumor activity ranging from tumor growth delay to regression. Consistent with the role of Akt in a survival pathway, GDC-0068 also enhanced antitumor activity of classic chemotherapeutic agents.

Conclusions: GDC-0068 is a highly selective, orally bioavailable Akt kinase inhibitor that shows pharmacodynamic inhibition of Akt signaling and robust antitumor activity in human cancer cells *in vitro* and *in vivo*. Our preclinical data provide a strong mechanistic rationale to evaluate GDC-0068 in cancers with activated Akt signaling. *Clin Cancer Res; 19(7); 1760–72. ©2012 AACR.*

Introduction

The serine/threonine kinase Akt (a.k.a. protein kinase B or PKB) is encoded by 3 closely related genes in humans, *Akt1* (PKB-α), *Akt2* (PKB-β), and *Akt3* (PKB-γ), that belong to the AGC family of kinases and share high homology with protein kinase A (PKA) and PKC. Akt is the central node of the PI3K–Akt–mTOR pathway and is negatively regulated by the tumor suppressor PTEN, a phospholipid phosphatase that counteracts the activity of phosphoinositide 3-kinase (PI3K). The products of PI3K activity, the lipid second messengers phosphatidylinositol (3,4,5) trisphosphate [$PI(3,4,5)P_3$] and $PI(3,4)P_2$, promote membrane association and activation of Akt. Akt is phosphorylated at 2 residues critical for its full activation: a threonine residue in the activation loop of the kinase domain (T308) by phosphoinositide-dependent kinase 1 (PDK1) and a serine residue within the hydrophobic motif of the regulatory domain (S473) that can be phosphorylated by a number of kinases, most prominently mTOR complex 2 (mTORC2; reviewed in ref. 1). Activated Akt phosphorylates and regulates the functions of numerous cellular proteins, including the FoxO proteins, mTOR complex 1 (mTORC1), and S6 kinase, thereby playing an essential role in cell proliferation, survival, growth, migration, and energy metabolism (2).

Activation of Akt constitutes a hallmark of a variety of human cancers (3, 4). Multiple mechanisms can lead to Akt activation in human cancers, among which the most frequent genetic alterations include loss of the tumor suppressor PTEN (5, 6), and mutational activation of the p110α catalytic subunit of PI3K (7, 8). Amplification of the genes encoding either Akt or PI3K has also been observed in a subset of human cancers (9, 10). In addition, mutations in

Authors' Affiliations: [1]Genentech, South San Francisco, California; and [2]Array BioPharma Inc., Boulder, Colorado

Note: Supplementary data for this article are available at Clinical Cancer Research Online (http://clincancerres.aacrjournals.org/).

J. Lin, D. Sampath, and M.A. Nannini contributed equally to this work and are joint first authors.

Corresponding Author: Kui Lin, Genentech, 1 DNA Way, South San Francisco, CA 94080. Phone: 650-225-8998; Fax: 650-225-1411; E-mail: klin@gene.com

doi: 10.1158/1078-0432.CCR-12-3072

Published OnlineFirst January 3, 2013; DOI: 10.1158/1078-0432.CCR-12-3072

Translational Relevance

Activation of Akt constitutes a hallmark of a variety of human cancers. Despite significant progress in identifying small-molecule inhibitors against Akt, selectivity profiles and dose-limiting toxicities of previously reported Akt inhibitors have raised concerns about their safety and mechanisms of action. GDC-0068 is a novel ATP-competitive Akt inhibitor currently in clinical trials. With impressive selectivity, GDC-0068 offers both a valuable tool to dissect Akt downstream signaling and cellular effects and a promising therapeutic agent to interrogate our hypotheses in the clinic. Consistent with its high selectivity and specific targeting of activated Akt, GDC-0068 not only shows dose-dependent inhibition of Akt signaling and robust antitumor activity, but also exhibits differential activity in cells with and without activated Akt signaling that is distinct from phosphoinositide 3-kinase (PI3K) inhibitors. These preclinical data suggest that a rational strategy can be applied to stratify patients likely to benefit in clinical trials with a potentially achievable therapeutic index.

Akt1 can result in its constitutive activation in diverse cancers (11, 12), and has recently been identified as the underlying genetic abnormality associated with the Proteus syndrome (13). Hyperactivation of Akt also occurs via deregulated signaling of many cell surface receptors, intracellular linkers, and signaling molecules, including amplification/mutation of the EGFR/ErbB growth factor receptor family members and oncogenic mutations in the RAS family (reviewed in ref. 14). Moreover, Akt activation has been associated with resistance to both chemotherapeutic agents and targeted agents (15). These observations make Akt an attractive target for anticancer drug discovery. The eventual success of drugs targeting the PI3K–Akt–mTOR pathway will depend on their therapeutic index and the ability to stratify patients likely to respond to these therapeutics.

The 3 isoforms of Akt have both overlapping and distinct functions and expression profiles (16, 17). Activation of all 3 Akt family members have been detected in a variety of human malignancies, and inducible short hairpin RNA (shRNA) knockdown studies suggest that inhibition of all 3 Akt isoforms is required for maximum efficacy in PTEN-deficient cancer xenograft models (18). Strategies for targeting Akt have included both ATP-competitive and allosteric compounds, several of which were or are being tested in clinical trials (19). Previously reported ATP-competitive inhibitors have significant off-target activity on other members of the AGC kinase family (20, 21), therefore challenges remain for the development of potent and selective inhibitors of Akt that are suitable as drug candidates. Here, we describe preclinical pharmacology and antitumor activity of a novel, highly selective, orally available ATP-competitive pan-Akt inhibitor GDC-0068. We show that GDC-0068 inhibits Akt signaling, leading to selective inhibition of cancer cell viability in a diagnostically defined subset of human cancer cells characterized by Akt activation. Consistent with the role of Akt in promoting cell survival, GDC-0068 also enhanced the efficacy of chemotherapeutic agents such as docetaxel and carboplatin. The antitumor activity of GDC-0068 was recapitulated in human cancer xenograft models representing a broad spectrum of tumor types. Our preclinical studies provide a strong mechanistic rationale for clinical development of GDC-0068 in the treatment of human cancer either as a single agent or in combination with standard of care chemotherapeutic drugs.

Materials and Methods

Cell culture

Cell lines were originally obtained from the American Type Culture Collection or from Deutsche Sammlung von Mikroorganismen und Zellkulturen GmbH cell bank and genotyped by Genentech's cell banking facility. Lines were cultured in Dulbecco's modified Eagle's medium (DMEM) or RPMI supplemented with 10% FBS at 37°C under 5% CO_2. MCF7-neo/HER2 ectopically expresses HER2 in the MCF7 parental cell line and was developed at Genentech (22). MCF10A isogenic cells were obtained from Horizon Discovery Ltd. (http://www.horizondiscovery.com) and maintained in MCF10A growth medium as described previously (23) in a 1:1 mixture of DMEM and F12 medium (DMEM–F12) supplemented with 5% horse serum, hydrocortisone (0.5 μg/mL), insulin (10 μg/mL), EGF (20 ng/mL), and 0.1 μg/mL cholera toxin. In cell viability assays, assay medium containing DMEM-F12 supplemented with 5% horse serum, hydrocortisone (0.5 μg/mL) was supplemented with either 20 or 0.2 ng/mL EGF.

Compounds and antibodies

GDC-0068, GDC-0941, and GDC-0980 were supplied by Genentech, Inc. Antibodies used include phospho-Akt^{Thr308}, phospho-Akt^{Ser473}, Akt, phospho-PRAS40^{Thr246}, phospho-FoxO1^{T24}/FoxO3^{T32}, phospho-S6$^{Ser235/236}$, phospho-S6$^{Ser240/242}$, phospho-4EBP1^{Ser65}, S6, PARP, cleaved PARP, and PTEN from Cell Signaling, a glyceraldehyde-3-phosphate dehydrogenase (GAPDH) antibody from Advanced ImmunoChemical and a β-actin antibody from Sigma.

Cell viability assays

The 384-well plates were seeded with 2,000 cells per well in a volume of 54 μL per well followed by incubation at 37°C under 5% CO_2 overnight (~16 hours). Compounds were diluted in dimethyl sulfoxide (DMSO) to generate the desired stock concentrations then added in a volume of 6 μL per well. All treatments were tested in quadruplicates. After 4 days incubation, relative numbers of viable cells were estimated using CellTiter-Glo (Promega) and total luminescence was measured on a Wallac Multilabel Reader (PerkinElmer). The concentration of drug resulting in IC_{50} was calculated from a 4-parameter curve analysis (XLfit, IDBS software) and was determined from a

Published OnlineFirst January 3, 2013; DOI: 10.1158/1078-0432.CCR-12-3072

minimum of 3 experiments. For cell lines that failed to achieve an IC_{50}, the highest concentration tested (10 μmol/L) is listed.

Protein assays

For immunoblots, cells were washed with cold PBS and lysed in 1× Cell Extraction Buffer (Biosource) supplemented with protease inhibitors (Roche), 1 mmol/L phenylmethylsulfonylfluoride (PMSF), and phosphatase inhibitor cocktails 1 and 2 from Sigma. Protein concentration was determined using the Bradford method (Bio-Rad). Equal protein amounts were separated by electrophoresis through Tris–glycine 4% to 20% gradient gels (Invitrogen) and proteins transferred onto nitrocellulose membranes. Primary antibodies were detected using IR Dye 800-conjugated (Rockland) and Alexa-Fluoro 680-conjugated (Molecular Probes) species-selective secondary antibodies. Detection and quantification were conducted using an Odyssey infrared scanner (LICOR) using the manufacturer's software.

Quantitative measurements of phospho and total Akt were conducted using a Luminex assay (Invitrogen) or a Meso Scale Discovery Multi-Spot Biomarker Detection System (Meso Scale Discovery). Phospho and total PRAS40 were quantified using a Luminex assay (Invitrogen) or a human ELISA kit (Invitrogen). Phospho and total S6 were quantified using a Meso Scale Discovery Multi-Spot Biomarker Detection System (Meso Scale Discovery).

Flow cytometry assays

For cell-cycle analyses, cells were trypsinized from the plates, fixed, and permeabilized by slowly dropping into cold 70% ethanol, then incubated overnight at −20°C. The cells were then washed with PBS and incubated in PBS containing 50 μg/mL propidium iodide (PI; Invitrogen) and 50 μg/mL RNaseA (Novagen) on ice for 30 minutes, and analyzed by flow cytometry. Cell-cycle distribution was determined using the ModFit software (Verity Software House). To detect apoptosis, cells were resuspended in PBS containing 4 mmol/L $CaCl_2$, 5% Annexin V -FITC (BD Pharmingen), and 5 μg/mL PI. The mixture was incubated on ice for 30 minutes and cells analyzed by flow cytometry (BD Biosciences).

Xenograft studies

In vivo efficacy was evaluated in multiple tumor cell line- and patient-derived xenograft models. Cells or tumor fragments were implanted subcutaneously into the flank of immunocompromised mice. Female or male nude (*nu/nu*) or severe combined immunodeficient mice (SCID)/beige mice were obtained from Charles River Laboratories, Harlan Laboratories, or Taconic. For the MCF7-neo/HER2 model, 17β-estradiol pellets (0.36 mg/pellet, 60-day release, no. SE-121; Innovative Research of America) were implanted into the dorsal shoulder before cell inoculation. The LuCaP35V patient-derived primary tumors were obtained from Dr. Robert Vessella at University of Washington (Seattle, WA; ref. 24); male mice were castrated before implantation of tumor fragments. After implantation of tumor cells or fragments into mice, tumors were monitored until they reached mean tumor volumes of 180 to 350 mm^3 and distributed into groups of 8 to 10 animals/group. GDC-0068 was formulated in 0.5% methylcellulose/0.2% Tween-80 (MCT) and administered daily (QD), via oral (*per os*; PO) gavage. Docetaxel (Sanofi Aventis) was formulated in 3% EtOH/97% saline and dosed intravenously (IV) every week (QW) at 2.5 or 7.5 mg/kg. Carboplatin (St. Mary's Pharmacy) was formulated in saline and dosed intraperitoneally (IP) weekly at 50 mg/kg.

Tumor volumes were determined using digital calipers (Fred V. Fowler Company, Inc.) using the formula $(L \times W \times W)/2$. Percentage tumor growth inhibition (%TGI) was calculated as the percentage of the area under the fitted curve (AUC) for the respective dose group per day in relation to the vehicle, such that $\%TGI = 100 \times [1 - (AUC_{treatment}/d)/(AUC_{vehicle}/d)]$. Curve fitting was applied to $\log_2$ transformed individual tumor volume data using a linear mixed-effects (LME) model with the R package nlme, version 3.1-97 in R v2.13.0 (R Development Core Team 2008; R Foundation for Statistical Computing; ref. 25). Tumor sizes and body weights were recorded twice weekly over the course of the study. Mice with tumor volumes $\geq$2,000 mm^3 or with losses in body weight 20% or more from their weight at the start of treatment were euthanized per Institutional Animal Care and Use Committee (IACUC) guidelines.

For pharmacodynamic marker analysis, xenograft tumors were excised from animals and immediately snap frozen in dry ice and LN_2. Frozen tumors were weighed and processed using a pestle (Scienceware) in 1× cell extraction buffer.

Immunohistochemistry

Immunohistochemisty (IHC) for cleaved caspase-3 (CC3) was carried out using 5-μm paraffin sections of formalin-fixed tissue on a VentanaBenchmark XT instrument (VMSI) by deparaffinization, treatment with antigen retrieval buffer (VMSI) and incubation with anti-CC3 primary antibody (Cell Signaling Technology) at 37°C. Bound antibody was detected using DABMap technology (VMSI) and sections were counterstained with hematoxylin.

Statistics

Significant differences (*P* values) comparing treatment data using cell lines with and without evaluated genetic abnormalities were determined by two-tailed Mann–Whitney test calculated using the JMP statistical software, version 5.1.2 (JMP Software).

Results

GDC-0068 blocked Akt signaling and showed antiproliferative and apoptosis-inducing effects in human cancer cell lines

GDC-0068 is an ATP-competitive inhibitor of Akt (Supplementary Fig. S1; ref. 26) and is equipotent against all 3 Akt isoforms, which share more than 95% sequence identity within the ATP-binding pocket, with potencies ranging from 5 to 18 nmol/L (Supplementary Table S1).

Published OnlineFirst January 3, 2013; DOI: 10.1158/1078-0432.CCR-12-3072

Because of the high degree of homology in the ATP-binding pockets among Akt, p70S6K, PKA and other members of the AGC family of kinases, selectivity against these kinases has been a challenge for the development of potent and specific Akt inhibitors. GDC-0068 showed more than 600 and more than 100-fold selectivity for Akt1 in IC_{50} against the closely related kinases PKA and p70S6K, respectively (Supplementary Table S1). When tested at 1 μmol/L in a panel of 230 protein kinases, which includes 36 human AGC family members, GDC-0068 inhibited only 3 other kinases by more than 70% at 1 μmol/L concentration (PRKG1α, PRKG1β, and p70S6K). IC_{50} values measured for these 3 kinases were 98, 69, and 860 nmol/L, respectively. Thus, with the exception of PKG1 (relative to which GDC-0068 is >10-fold more selective for Akt1), GDC-0068 displays a more than 100-fold selectivity for Akt1 over the next most potently inhibited non-Akt kinase, p70S6K, in the screening kinase panel (Supplementary Table S1; ref. 26).

The biologic activity of GDC-0068 was evaluated in cell-based assays *in vitro*. Similar to other ATP-competitive Akt inhibitors (21, 27, 28), GDC-0068 induced a dose-dependent increase in Akt phosphorylation at both Thr^{308} (T308) and Ser^{473} (S473) residues in all cell lines tested, including lines in which the PI3K/Akt pathway is activated, such as PC-3 (PTEN homozygous deletion mutant, prostate), BT474M1 (PIK3CA^{K111N} mutant and HER2-amplified, breast), IGROV-1 (PTEN$^{T319fsX1/Y155C}$ and PIK3CA^{*1069W}, ovarian; Fig. 1A). As we and others have shown, binding of the ATP competitive inhibitors to the active site of Akt can protect these sites from phosphatases, leading to increased pAkt (29). Despite this increase in pAkt, downstream Akt signaling activity was inhibited in a dose-dependent manner as shown by the diminished phosphorylation of the proline-rich Akt Substrate of 40 kDa (PRAS40) within 15 minutes of treatment (Fig. 1A). Maximum inhibition of pPRAS40 was achieved within 1 hour, with IC_{50} values of approximately 200 nmol/L in multiple cancer cell lines (Supplementary Table S1). Phosphorylation of other downstream targets, such as FoxO1 and FoxO3a, 4EBP1 and S6, were also inhibited in a dose- and time-dependent manner (Fig. 1A and B). Inhibition of pS6, the substrate of p70S6K that is further downstream of Akt, exhibited a delayed response compared with the proximal Akt targets, such as pPRAS40 (Fig. 1B).

The effects of GDC-0068 on cell-cycle progression and cell death were also assessed in cancer cell lines in which the PI3K/Akt pathway is activated, including PC-3, BT474M1, and the MCF7-neo/HER2 (PIK3CA^{E545K} mutant stably expressing a HER2 transgene) breast cancer cell lines (25). A dose-dependent increase in the G_0–G_1 phase population was observed in all cell lines tested (Fig. 2A and Supplementary Fig. S2A). This effect was apparent within 15 hours of treatment and persisted for at least 72 hours in the

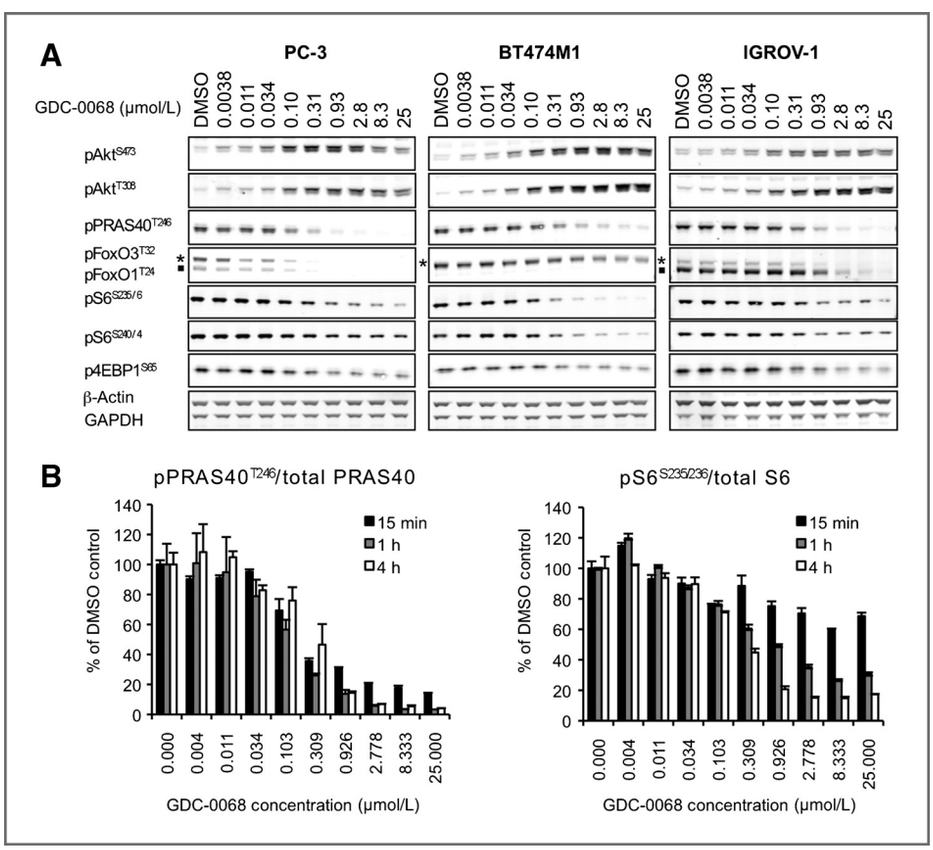

Figure 1. Dose-dependent effect of GDC-0068 on Akt pathway biomarkers. A, Western blot analysis of phospho biomarkers in response to increasing concentrations of GDC-0068 in PC-3, BT474M1, and IGROV-1 cell lines after 1 hour of treatment. The expected positions of pFoxO3^{T32} and pFoxO1^{T24}, which were detected with the same antibody, were indicated with an asterisk and a dot, respectively. B, quantification of dose-dependent effect of GDC-0068 on pPRAS40 (by the Luminex assay) and pS6 (by the meso scales assay) levels in PC-3 cells after 15 minutes, 1 hour, or 4 hours of treatment. Ratios of each phosphorylated protein to total protein were expressed as percentage of the ratio obtained from cells treated with DMSO vehicle control. Error bars represent SEM from 3 experiments.

Published OnlineFirst January 3, 2013; DOI: 10.1158/1078-0432.CCR-12-3072

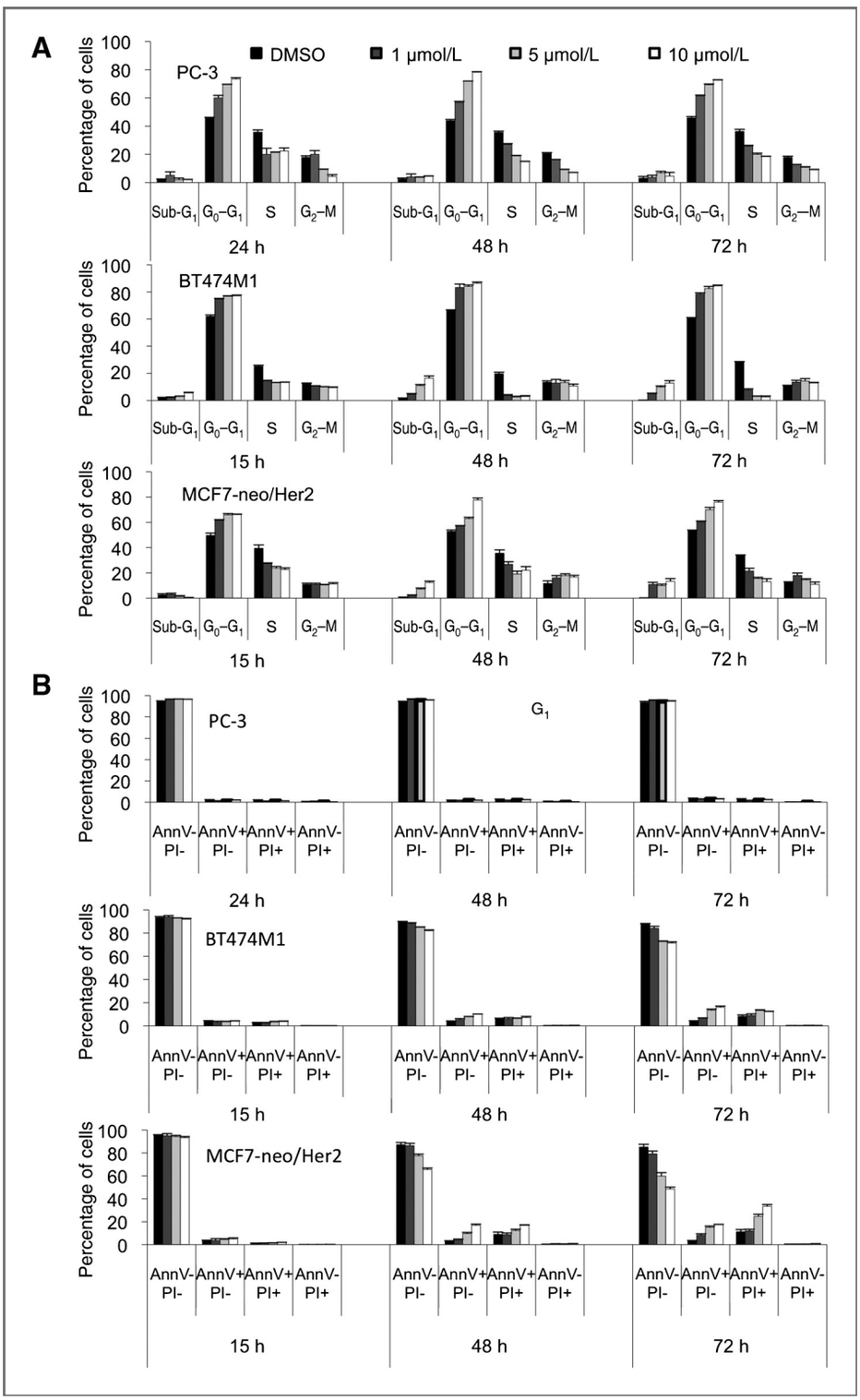

Figure 2. Effects of GDC-0068 on cell-cycle progression and apoptosis in cancer cell lines. A, effect of GDC-0068 on cell-cycle distribution in PC-3, MCF7-neo/HER2, and BT474M1 cells. B, effect of GDC-0068 on apoptotic response analyzed by Annexin V/PI staining in PC-3, MCF7-neo/HER2, and BT474M1 cells. Cells were incubated with DMSO or GDC-0068 at 1, 5, or 10 μmol/L. Cell-cycle distribution or apoptosis was analyzed at 15 (24 hours for PC-3), 48, and 72 hours. Error bars represent SEM from triplicates.

presence of GDC-0068. A dose-dependent increase in the sub-G_1 peak was also observed in BT474M1 and MCF7-neo/HER2 cells by 48 hours of treatment (Fig. 2A). Similarly, Annexin V/PI staining indicated that GDC-0068 treatment caused a dose- and time-dependent increase in apoptotic and necrotic populations in BT474M1 and MCF7-neo/HER2 cells, but not in PC-3 cells (Fig. 2B and Supplementary Fig. S2B).

Published OnlineFirst January 3, 2013; DOI: 10.1158/1078-0432.CCR-12-3072

High Akt activity predicts sensitivity to GDC-0068

Consistent with its effect on cell-cycle progression and apoptosis, GDC-0068 exhibited dose-dependent inhibition of overall viability in multiple cancer cell lines (Fig. 3A and Supplementary Table S2). In a panel of 100 cell lines, we determined IC_{50} values on cell viability in response to GDC-0068. To investigate potential biomarkers that may predict response to GDC-0068, we also determined baseline $pAkt^{S473}$ levels in these cell lines, as well as mutational status of key components in cancer signaling pathways including loss or mutation of the tumor suppressor PTEN, mutations in PI3K, amplification of HER2, or mutations in the *KRAS* or *BRAF* oncogenes. Sensitivity to GDC-0068 was strongly associated with pAkt levels above the median value ($P = 1.8 \times 10^{-7}$), and cells with loss of PTEN protein or genetic mutations in PTEN were also significantly more sensitive to GDC-0068 than those without ($P = 7.1 \times 10^{-5}$). Cells with PIK3CA mutations did not show significantly increased overall sensitivity to GDC-0068 compared with PIK3CA wild-type (WT) cells ($P = 0.14$); however, mutations in the kinase domain (e.g., H1047R; ref. 8) were significantly associated with increased sensitivity ($P = 0.002$), whereas helical (e.g., E545K) and other domain (e.g., I391M) mutations did not show significant association ($P = 0.75$). Conversely, mutations in KRAS or BRAF were associated with resistance to GDC-0068 ($P =$

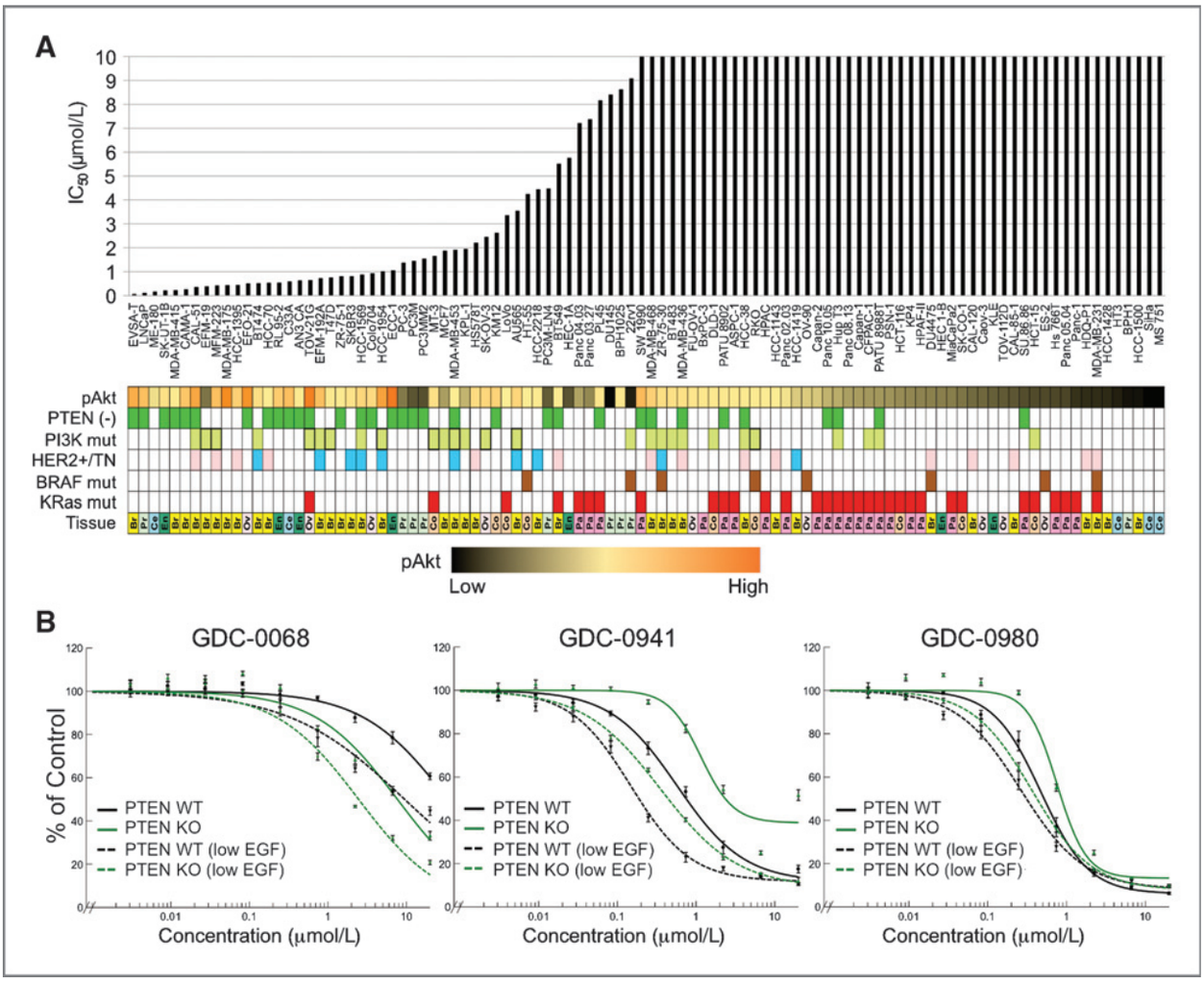

Figure 3. Effect of GDC-0068 on cell viability in a panel of cancer cell lines and MCF10A cells isogenic at the PTEN locus. A, IC_{50} values of GDC-0068 on cell viability sorted from low to high in a panel of 100 cancer cell lines. pAkt levels, known genetic alterations in the indicated biomarkers, as well as tissue origins are indicated as a colored box under each cell line: pAkt levels are represented by a heatmap; PTEN (−), PTEN loss by Western blot analysis or mutated, green; PI3K mut, PIK3CA mutated, honeydew (those with kinase domain mutations are indicated with a bolded border); HER2+, HER2-amplified or overexpressed breast cancer cell lines, blue; TN, triple-negative breast cancer lines, pink; BRAF mut, BRAF mutated, brown; KRAS mut, KRAS mutated, red. Tissue origins for each cell line are indicated in different colors with letters indicating breast (Br), cervical (Ce), colon (Co), endometrial (En), ovarian (Ov), pancreatic (Pa), and prostate (Pr). B, dose–response curves of 3 different PI3K pathway inhibitors on the viability of isogenic MCF10A cells with or without PTEN knockout (KO), in assay medium containing either 20 ng/mL EGF or 0.2 ng/mL EGF (low EGF). Error bars represent SEM from quadruplicates. Representative data from more than 3 independent experiments are shown.

Published OnlineFirst January 3, 2013; DOI: 10.1158/1078-0432.CCR-12-3072

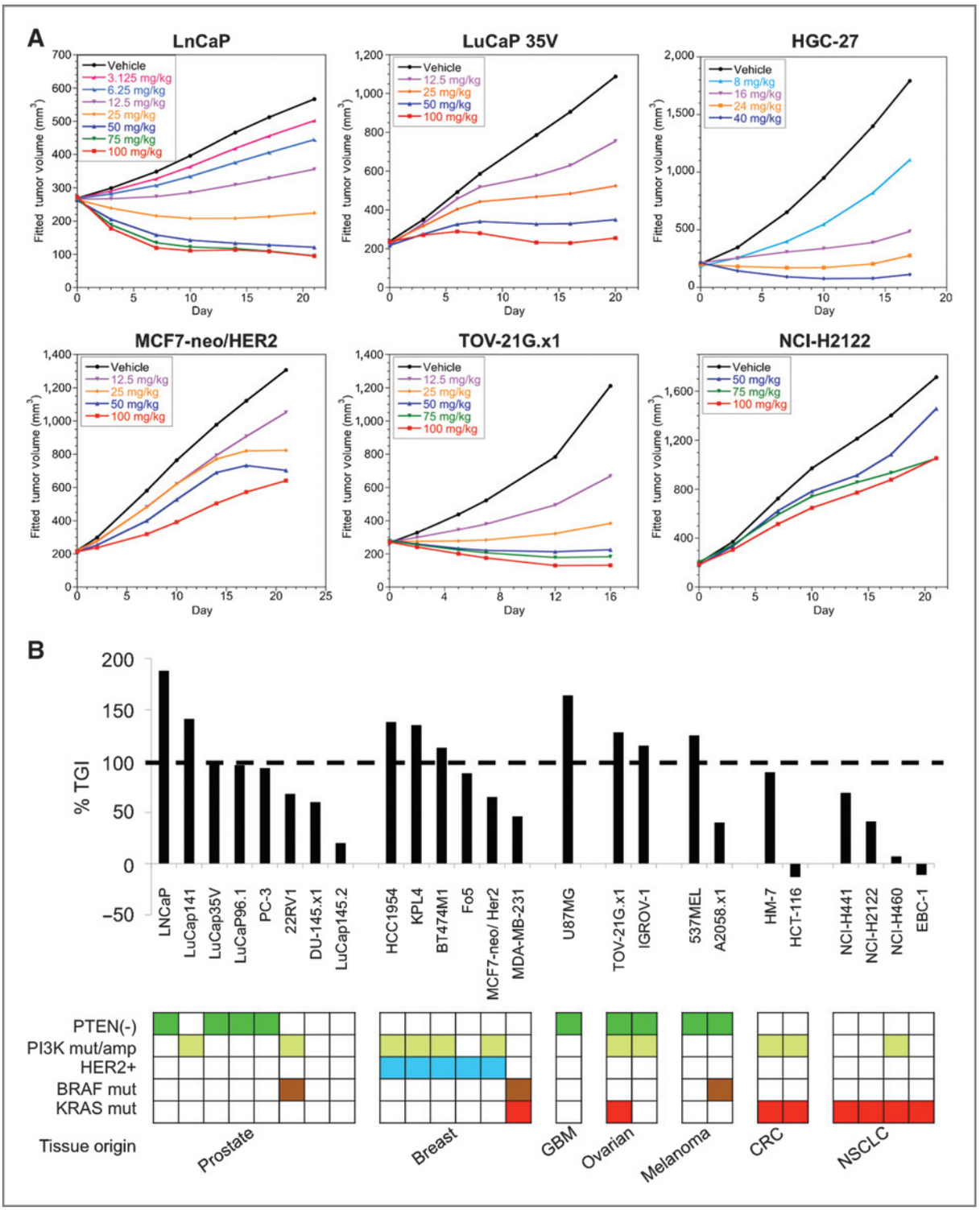

Figure 4. Single agent efficacy of GDC-0068 in human tumor xenograft models. A, fitted tumor volume dose–response plots of GDC-0068 treatment in the following xenograft models: LNCaP (PTEN-null, androgen-sensitive AR^+ prostate cancer cell line), LuCaP 35V (PTEN-low, primary patient-derived androgen-independent AR^+ prostate cancer xenograft), HGC-27 ($PTEN^-$-null gastric cancer cell line), MCF7-neo/HER2 ($PIK3CA^{E545K}$, HER2 overexpressed breast cancer cell line), TOV-21G.x1 (PTEN-null, $PIK3CA^{H1047R}$, $KRAS^{G13C}$ ovarian cancer cell line), and NCI-H2122 ($KRAS^{G12C}$ NSCLC cell line). B, comparison of %TGI in multiple tumor xenograft models at day 21 after daily oral treatment with 100 mg/kg of GDC-0068. Dashed line demarcates tumor stasis, which is defined as 100% TGI. Tumor growth delay increases from 0% to 100% TGI, and more than 100% TGI indicates tumor regression. PTEN(−), PTEN-null or PTEN-low by Western blot analysis or IHC; PI3K mut/amp, PIK3CA mutated or amplified; HER2+, HER2-amplified or overexpressed; BRAF mut, BRAF mutated; KRAS mut, KRAS mutated. Tissue origins are also indicated.

Published OnlineFirst January 3, 2013; DOI: 10.1158/1078-0432.CCR-12-3072

1.0×10^{-7}); in cells with these mutations the correlation of sensitivity with high pAkt or PTEN-deficiency was often lost, such as in the pancreatic cell lines. In addition, triple-negative breast cancer cell lines tended to be less sensitive to GDC-0068 than $HER2^+$ or ER^+ breast cancer cell lines ($P = 0.018$), likely reflecting the enrichment of an activated RAS pathway gene expression signature in this subset of breast cancers (30).

These data are consistent with previous reports that loss of PTEN strongly correlates with Akt activation (31). Indeed, higher pAkt levels were significantly associated with PTEN loss or mutation in our panel (mean pAkt levels = 11.44 arbitrary units in PTEN deficient cells vs. 4.85 in others cell lines; $P = 0.00016$), and with PIK3CA kinase domain mutants (mean pAkt levels = 13.32 in kinase domain mutants vs. 6.32 in all other mutant or WT cell lines; $P = 0.013$) but not with other nonkinase domain PI3K mutants (mean pAkt levels = 7.63 vs. 6.02 in PIK3CA WT cells; $P = 0.45$). To further determine whether PTEN loss can result in increased sensitivity to GDC-0068, we evaluated nontransformed human mammary epithelial cells, MCF10A, with their isogenic PTEN knockout counterparts (23). Cells were grown in regular MCF10A growth medium, and assayed for dose–response to GDC-0068 in assay medium containing either 20 ng/mL EGF or 0.2 ng/mL EGF (low EGF; Fig. 3B). Although very little pAkt was detectable in the parental MCF10A cells, Akt phosphorylation at both S473 and T308 were markedly elevated in the PTEN knockout cells under both conditions, along with increased phosphorylation of Akt downstream targets such as PRAS40 and S6 (Supplementary Fig. S3). The parental nontransformed MCF10A cells were quite resistant to GDC-0068 under the high EGF condition, with only 39% maximum inhibition of viability at concentrations up to 20 μmol/L of GDC-0068 (Fig. 3B). Reducing EGF increased sensitivity to 55% maximum inhibition in the parental line. Loss of PTEN resulted in a leftward shift of the dose–response curves under both conditions, with maximum inhibitions of 67% and 79% under high and low EGF conditions, respectively. A greater than 4-fold decrease in IC_{50} values was observed under low EGF conditions in PTEN knockout versus WT cells (1.8 vs. 7.3 μmol/L, respectively), and a greater than 3.5-fold decrease in IC_{50} values was observed under high EGF conditions in PTEN knockout versus WT cells (5.7 vs. > 20 μmol/L, respectively; Fig. 3B).

The strong correlation of GDC-0068 sensitivity with PTEN loss is in contrast to the previous reports in which no significant correlation with PTEN loss was observed for sensitivity to other PI3K-targeting inhibitors including the class I PI3K inhibitor GDC-0941 (32, 33) and dual PI3K/mTOR inhibitor GDC-0980 (25) but is consistent with another ATP-competitive inhibitor AZD5363 reported recently (20). We therefore examined the sensitivity of the MCF10A PTEN isogenic cells to the PI3K inhibitor GDC-0941 and the PI3K/mTOR inhibitor GDC-0980. Both inhibitors were more potent at inhibiting the parental MCF10A cells than GDC-0068 (Fig. 3B). However, in direct contrast to GDC-0068, PTEN loss resulted in a 3-fold increase in IC_{50} for GDC-0941 (0.78 vs. 2.3 μmol/L) under high EGF conditions and 2-fold increase (0.20 vs. 0.44 μmol/L) under low EGF conditions, respectively. Smaller increases in GDC-0980 IC_{50} were also observed under both conditions. Together, these data indicate that PTEN-loss in MCF10A cells increased sensitivity to the Akt inhibitor GDC-0068, whereas decreased sensitivity to PI3K inhibitors. This is consistent with the hypothesis that Akt activation becomes less dependent on PI3K activity upon PTEN-loss, and that activated Akt is preferentially targeted by ATP-competitive inhibitors such as GDC-0068 (29).

GDC-0068 is efficacious in a broad spectrum of human cancer xenograft models

The *in vitro* sensitivity profile of GDC-0068 was recapitulated *in vivo* in xenograft models representing a spectrum of cancer types including prostate, breast, ovarian, colorectal, non–small cell lung, glioblastoma, and melanoma (Fig. 4A and B). GDC-0068 was typically efficacious in xenograft models in which Akt was activated because of genetic alterations including PTEN loss, PIK3CA mutations/amplifications, or HER2 overexpression. In these models, tumor growth delay, stasis, or regression was achieved at or below 100 mg/kg daily oral dose, which was the maximum dose tested in immunocompromised mice that was well tolerated. In contrast, cancer cell lines and xenograft models that harbor mutations in KRAS or BRAF, such as the $KRAS^{G12C}$ mutant NCI-H2122 non–small cell lung carcinoma (NSCLC) or the $KRAS^{G12D}$ and $PIK3CA^{H1047R}$ mutant HCT-116 colorectal cancer (CRC) model, were less sensitive to GDC-0068 both *in vitro* and *in vivo*, even in models with a coexisting PIK3CA mutation (Figs. 3A, 4A and B). Interestingly, an ovarian cancer cell line that contains both PTEN loss and the $PIK3CA^{H1047R}$ hot-spot mutation, TOV-21G and its *in vivo* selected subline TOV-21G.x1, remained exquisitely sensitive to GDC-0068 both *in vitro* and *in vivo* despite the presence of the $KRAS^{G13C}$ mutation (Figs. 3A, 4A and B and Supplementary Table S2), suggesting that Akt activity is indispensible for cell viability in this line. Single agent treatment of GDC-0068 was well tolerated with less than 10% body weight loss observed compared with vehicle controls in all models tested *in vivo* (Supplementary Table S3).

The relationship between pharmacokinetics (PK) and pharmacodynamics (PD) of GDC-0068 was investigated in 3 xenograft models that showed dose-dependent response to drug treatment: MCF7-neo/HER2, TOV-21G.x1, and LNCaP (Fig. 4A). The mean *in vitro* cell viability IC_{50} of GDC-0068 in these 3 cell lines is 2.56, 0.44, and 0.11 μmol/L, respectively. The phosphorylation levels of Akt, PRAS40, and S6 in MCF7-neo/HER2 tumors, as well as plasma and tumor concentrations of GDC-0068, were evaluated over 24 hours following a single dose of GDC-0068 at 0, 12.5, 50, or 100 mg/kg (Fig. 5A). Within 0.5 hour, a dose-dependent increase in Akt phosphorylation at both T308 and S473 sites was observed, reaching maximal levels between 4 and 8 hours. The kinetics of pAkt levels correlated better with GDC-0068 drug kinetics in tumors than in

Published OnlineFirst January 3, 2013; DOI: 10.1158/1078-0432.CCR-12-3072

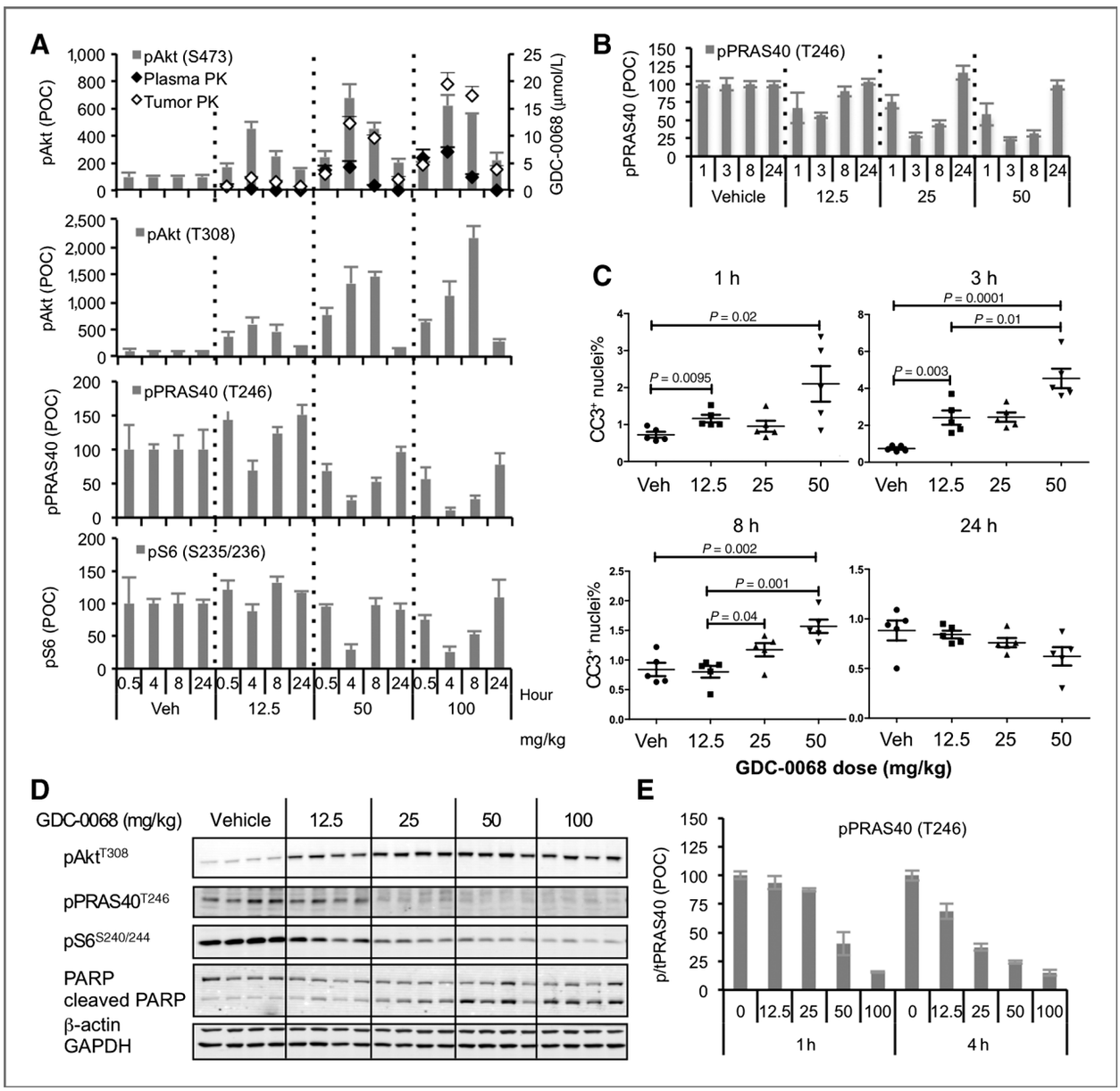

Figure 5. Pharmacokinetic (PK) and pharmacodynamic (PD) relationship of GDC-0068 in xenograft models. A, pAkt^{S473}, pAkt^{T308}, pPRAS40^{T246}, pS6$^{S235/236}$ levels (gray bars) in MCF7-neo/HER2 tumors at 0.5, 4, 8, and 24 hours following a single dose of GDC-0068 at 12.5, 50, or 100 mg/kg or vehicle. Corresponding plasma (closed diamonds) and tumor (open diamonds) concentrations of GDC-0068 are also plotted on a second axis. Phosphorylated protein levels are quantitated by Western blot analyses and normalized to GAPDH levels, then expressed as percentage of vehicle control (POC). Error bars represent SEM for tumor samples from 4 different animals. B, pPRAS40^{T246} levels in TOV-21G.x1 tumors at 1, 3, 8, and 24 hours after a single dose of GDC-0068 at 12.5, 25, or 50 mg/kg or vehicle. Phosphorylated protein levels are quantified by Western blot analyses and normalized to GAPDH levels, then expressed as percentage of vehicle control (POC). Error bars represent SEM for tumor samples from five different animals. C, quantification of CC3-positive (CC3$^+$) nuclei by IHC in TOV-21G.x1 tumors at 1, 3, 8, and 24 hours following a single dose of GDC-0068 at 12.5, 25, or 50 mg/kg or vehicle. Error bars represent SEM for tumor samples from 5 different animals. D, Western blot analysis of the indicated biomarkers in LNCaP tumors at 4 hours following a single dose of GDC-0068 at 12.5, 25, 50, or 100 mg/kg or vehicle. E, quantification of pPRAS40^{T246} levels in LNCaP tumors at 1 and 4 hours after a single dose of GDC-0068 at 12.5, 25, 50, or 100 mg/kg or vehicle. pPRAS40^{T246} levels were measured by ELISA and normalized to total PRAS40 levels, then expressed as percentage of vehicle control (POC). Error bars represent SEM for tumor samples from 4 different animals.

mouse plasma, given the higher levels of GDC-0068 in tumors compared with plasma beyond 4 hours due to rapid distribution of GDC-0068 from plasma to the tumor (Fig. 5A). Correlating closely with the increase in pAkt levels, a dose- and time-dependent decrease in phosphorylated PRAS40 at Thr^{246} was observed, with more than 50% knockdown associated with 50 and 100 mg/kg of GDC-0068, which was sustained up to 8 hours. Phosphorylation

Published OnlineFirst January 3, 2013; DOI: 10.1158/1078-0432.CCR-12-3072

of S6 at Ser^{235} and/or Ser^{236} was also inhibited in a dose- and time-dependent manner, albeit with delayed kinetics consistent with the distal nature of this biomarker downstream of Akt. The tumor pharmacodynamics effect of GDC-0068 was also analyzed in the TOV-21G.x1 ovarian cancer xenograft model. Similar to observations in the MCF7-neo/HER2 xenograft model, a dose-dependent reduction in $pPRAS40^{T246}$ was observed in the TOV-21G.x1 tumors with 50% or more reduction sustained between 3 to 8 hours when animals were dosed with 25 and 50 mg/kg GDC-0068 (Fig. 5B).

GDC-0068 elicited tumor stasis at 25 mg/kg in the TOV-21G.x1 model, with partial regressions observed at 50 mg/kg or higher, suggesting a strong dependence on Akt signaling in this model (Fig. 4A). To further investigate the mechanism of GDC-0068–mediated TGI, the level of CC3 was determined by IHC in the TOV-21G.x1 tumors treated with GDC-0068. A significant increase in nuclear CC3 was observed within 1 hour, with maximum levels observed at 3 hour in the 50 mg/kg group (Fig. 5C and Supplementary Fig. S4). Substantial tumor regression was also observed in the PTEN-null prostate cancer model LNCaP with 50 mg/kg or higher doses of GDC-0068 (Fig. 4A). Induction of apoptosis was also evidenced by a dose-dependent increase in the cleavage of PARP within 4 hours postdose, correlating with inhibition of $pPRAS40^{T246}$ and $pS6^{S240/244}$ in this model (Fig. 5D and E). Thus, efficacy of GDC-0068 in xenograft models is associated with efficient inhibition of Akt signaling nodes and induction of cell death in the sensitive models.

GDC-0068 enhanced the antitumor activity of chemotherapeutic agents

Akt activation has been associated with resistance to chemotherapeutic agents (15). We hypothesized that inhibiting Akt activity with GDC-0068 would overcome resistance or enhance the antitumor activity of standard of care chemotherapeutic drugs. Indeed, combination of multiple chemotherapeutic agents with GDC-0068 resulted in combination index (CI) values below 0.8 in the majority of cancer cell lines tested (as determined by the Chou and Talalay method; ref. 34), suggesting synergism for most of the combinations (Supplementary Fig. S5A). Interestingly, MCF10A cells with isogenic knockin of the activating PIK3CA mutation H1047R exhibited decreased sensitivity to docetaxel compared with the WT parental cells (Supplementary Fig. S5B). Combination with GDC-0068 resulted in significantly increased inhibition of cell viability in both PIK3CA WT and H1047R mutants compared with each single agent alone, suggesting Akt activation contributes to the resistance to docetaxel (Supplementary Fig. S5C).

When tested *in vivo*, daily dosing of GDC-0068 in combination with docetaxel induced tumor regression and stasis in the PC-3 and MCF7-neo/HER2 xenograft models, at doses where each single agent was ineffective or only caused modest tumor growth delay (Fig. 6A and B). Similarly, increased TGI was observed in the OVCAR3 ovarian cancer xenograft model when GDC-0068 was combined with carboplatin (Fig. 6C). The combination of GDC-0068 with docetaxel or carboplatin was tolerated with less than 5% body weight loss when compared with treatment with each chemotherapeutic agent alone (Supplementary Table S3).

Discussion

Identified 2 decades ago, the serine/threonine kinase Akt has emerged as a promising target for drug development. Akt is critically involved in multiple signaling cascades, controlling cell growth and proliferation, and its activation is a prominent feature of many human cancers. On the basis of the strong rationale for targeting Akt for cancer therapy, multiple attempts to identify Akt inhibitors with acceptable pharmaceutical properties have been pursued (17). However, despite the significant progress in identifying Akt small-molecule inhibitors, selectivity has been a key issue for many previously reported ATP-competitive Akt inhibitors (relative to the kinome, especially within the AGC kinase family), raising concerns on safety and unclear mechanisms of action of these drugs. Even allosteric inhibitors, which held the promise of greater selectivity against the kinome, have been reported to exhibit unexpected nonkinase off-target effects (35).

GDC-0068 is a highly selective, orally available pan-Akt inhibitor discovered through a structure-based drug discovery approach guided by cocrystal structures of ATP-competitive inhibitors in complex with Akt1 and the closely related PKA (26). It exhibited unprecedented selectivity against the kinome, including AGC family members previously shown to be significantly inhibited by other ATP-competitive inhibitors (20, 21). Our preclinical work presented in this report shows that GDC-0068 effectively inhibited Akt signaling to downstream biomarkers and dose-dependently decreased tumor cell viability in a broad spectrum of tumor models *in vitro* and *in vivo*. Moreover, we observed a strong association between cellular sensitivity to GDC-0068 and baseline levels of Akt activation. Genetic alterations that lead to Akt activation, most notably PTEN loss and PIK3CA kinase domain mutations, also showed positive correlation with sensitivity to GDC-0068, whereas mutations in KRAS or BRAF were negative predictors of GDC-0068 sensitivity. Interestingly, while PTEN-loss decreased sensitivity to PI3K inhibitors GDC-0941 and GDC-0980 in PTEN knockout MCF10A cells compared with the isogenic parental cells, it increased the sensitivity of these cells to GDC-0068, which is consistent with the notion that PTEN-loss reduces the dependence of Akt activation on PI3K activity and promotes cell proliferation in an Akt-dependent manner. Lessons learned from clinical experiments have indicated that broad and potent preclinical activity does not necessarily translate into clinical success without acceptable therapeutic index. As an ATP-competitive inhibitor, selective targeting of activated Akt is expected to further increase GDC-0068's effectiveness in cells with high pAkt levels (29), such as tumor cells with PTEN-loss (31), whereas decrease its potency in cells with low Akt activity, such as normal cells, thereby

Published OnlineFirst January 3, 2013; DOI: 10.1158/1078-0432.CCR-12-3072

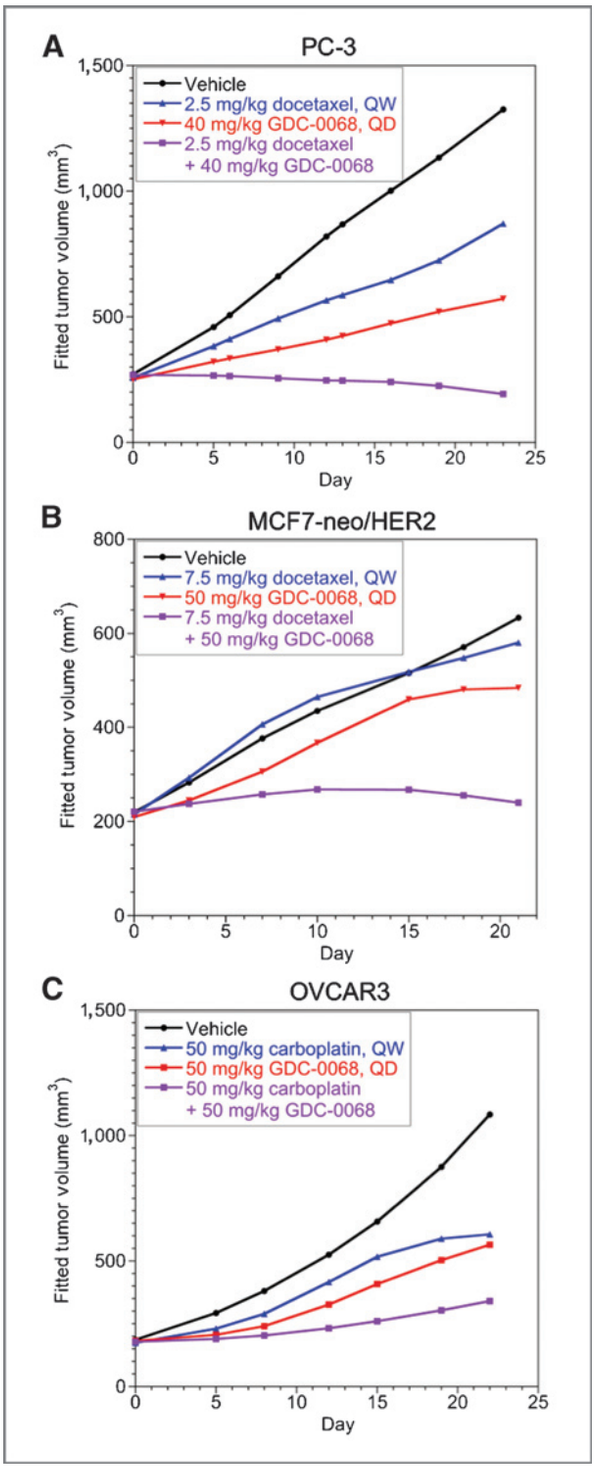

Figure 6. Efficacy of GDC-0068 in combination with docetaxel or carboplatin in human tumor xenograft models. A, PC-3 prostate xenografts treated with GDC-0068 administered at 50 mg/kg orally and daily (PO and QD) and docetaxel at 2.5 mg/kg IV once a week for 3 weeks (QW × 3). B, MCF7-neo/HER2 breast cancer xenografts, treated with GDC-0068 dosed at 50 mg/kg PO and QD and docetaxel at 7.5 mg/kg IV QW × 3. C, OVCAR3 ovarian cancer xenografts treated with GDC-0068 at 50 mg/kg PO and QD and carboplatin at 50 mg/kg IP QW × 3.

potentially widen its therapeutic index. Interestingly, different safety profiles have been observed between allosteric and ATP-competitive inhibitors in the clinic, for example, rash is reported as a dose-limiting toxicity for the allosteric inhibitor MK2206 but not several ATP-competitive Akt inhibitors including GDC-0068 (36–38), raising the possibility that differences in on-target effects on normal cells could exist between the 2 classes of inhibitors due to their different mechanisms of action.

In xenograft models, GDC-0068 was efficacious as a single agent when administered orally in models with genetic alterations that are predicted to cause activation of Akt, consistent with our *in vitro* results. The maximum antitumor effect of GDC-0068 achieved in the PC-3 xenograft model was comparable with the TGI generated by inducible shRNA knockdown of all 3 Akt isoforms in this model (18), consistent with an on-target drug effect. We also confirmed the efficacy of GDC-0068 in more clinically relevant disease models such as the patient-derived androgen-independent prostate cancer primary xenograft model LuCaP35V, which expresses reduced levels of the PTEN protein. Collectively, GDC-0068 shows single agent and on-target activity in tumor models in which the Akt pathway is activated.

Analysis of GDC-0068 pharmacokinetics revealed dose-dependent plasma and tumor exposure. GDC-0068 caused an increase in pAkt levels even at subefficacious doses and the kinetics of pAkt increase correlated with tumor drug levels. This is consistent with our finding that ATP-competitive inhibitors lock Akt in a hyperphosphorylated yet nonfunctional state by preventing the accessibility of phosphatases (29), and as such, pAkt increase is a direct indicator of GDC-0068 binding to Akt. At efficacious doses a 50% to 75% suppression of the Akt substrate pPRAS40 and the downstream target pS6 was observed, showing inhibition of Akt signaling is necessary for robust antitumor responses *in vivo*. However, the degree of TGI varies between different models, with responses ranging from tumor growth delay to tumor regression even in the presence of comparable pPRAS40 suppression. The latter suggests that genetic background of each tumor model determines the dependence of tumor growth on Akt signaling.

Akt is known to be critically involved in glucose metabolism (15), and indeed we observed a transient, completely reversible increase in glucose and insulin levels in preclinical models after GDC-0068 treatment (data not shown), consistent with an on-target effect on Akt. Details of these data will be discussed elsewhere.

In summary, GDC-0068 is a novel, highly selective ATP-competitive Akt inhibitor with compelling selectivity, efficacy, and oral pharmacokinetics that support its clinical development as an anticancer agent either singly or in combination with chemotherapeutic agents. The selective activity of GDC-0068 in cancer cells with activated Akt signaling allows for a rational strategy to identify patients who will potentially benefit in clinical trials, which are currently underway.

Published OnlineFirst January 3, 2013; DOI: 10.1158/1078-0432.CCR-12-3072

Disclosure of Potential Conflicts of Interest

J. Lin, D. Sampath, M.A. Nannini, B.B. Lee, M. Degtyarev, J. Oeh, H. Savage, Z. Guan, R. Hong, R. Kassees, L.B. Lee, B.M. Liederer, H. Koeppen, N. J. Skelton, J.J. Wallin, M. Belvin, E. Punnoose, L.S. Friedman, and K. Lin are employees of Genentech, a member of the Roche Group, and have ownership interest (including patents) in it. S. Gross has ownership interest (including patents) in Array Biopharma. T. Risom disclosed no potential conflicts of interest.

Authors' Contributions

Conception and design: D. Sampath, M.A. Nannini, M. Degtyarev, B.M. Liederer, N.J. Skelton, J.J. Wallin, L.S. Friedman, K. Lin
Development of methodology: J. Lin, M.A. Nannini, M. Degtyarev, T. Risom, S. Gross, K. Lin
Acquisition of data (provided animals, acquired and managed patients, provided facilities, etc.): J. Lin, M.A. Nannini, B.B. Lee, M. Degtyarev, J. Oeh, H. Savage, Z. Guan, R. Hong, R. Kassees, S. Gross, H. Koeppen, J.J. Wallin, E. Punnoose, L.S. Friedman
Analysis and interpretation of data (e.g., statistical analysis, biostatistics, computational analysis): J. Lin, M.A. Nannini, B.B. Lee, M. Degtyarev, R. Hong, R. Kassees, L.B. Lee, T. Risom, B.M. Liederer, H. Koeppen, J.J. Wallin, E. Punnoose, K. Lin
Writing, review, and/or revision of the manuscript: J. Lin, D. Sampath, M.A. Nannini, M. Degtyarev, T. Risom, B.M. Liederer, H. Koeppen, N.J. Skelton, J.J. Wallin, M. Belvin, E. Punnoose, L.S. Friedman, K. Lin
Administrative, technical, or material support (i.e., reporting or organizing data, constructing databases): M. Degtyarev, J. Oeh, H. Savage, K. Lin
Study supervision: D. Sampath, M.A. Nannini, K. Lin

Acknowledgments

The authors thank the *In Vivo* Cell Culture core facility and dosing technicians in the Department of Translational Oncology for their support in conducting efficacy studies. The authors also thank the members of the Akt inhibitor project teams at Array BioPharma and Genentech for the development of GDC-0068.

The costs of publication of this article were defrayed in part by the payment of page charges. This article must therefore be hereby marked *advertisement* in accordance with 18 U.S.C. Section 1734 solely to indicate this fact.

Received September 27, 2012; revised December 11, 2012; accepted December 14, 2012; published OnlineFirst January 3, 2013.

References

1. Bhaskar PT, Hay N. The two TORCs and Akt. Dev Cell 2007;12:487–502.
2. Manning BD, Cantley LC. AKT/PKB signaling: navigating downstream. Cell 2007;129:1261–74.
3. Robey RB, Hay N. Is Akt the "Warburg kinase"?-Akt-energy metabolism interactions and oncogenesis. Semin Cancer Biol 2009;19:25–31.
4. Bellacosa A, Kumar CC, Di Cristofano A, Testa JR. Activation of AKT kinases in cancer: implications for therapeutic targeting. Adv Cancer Res 2005;94:29–86.
5. Li J, Yen C, Liaw D, Podsypanina K, Bose S, Wang SI, et al. PTEN, a putative protein tyrosine phosphatase gene mutated in human brain, breast, and prostate cancer. Science 1997;275:1943–7.
6. Steck PA, Pershouse MA, Jasser SA, Yung WK, Lin H, Ligon AH, et al. Identification of a candidate tumour suppressor gene, MMAC1, at chromosome 10q23.3 that is mutated in multiple advanced cancers. Nat Genet 1997;15:356–62.
7. Shayesteh L, Lu Y, Kuo WL, Baldocchi R, Godfrey T, Collins C, et al. PIK3CA is implicated as an oncogene in ovarian cancer. Nat Genet 1999;21:99–102.
8. Samuels Y, Wang Z, Bardelli A, Silliman N, Ptak J, Szabo S, et al. High frequency of mutations of the PIK3CA gene in human cancers. Science 2004;304:554.
9. Staal SP. Molecular cloning of the akt oncogene and its human homologues AKT1 and AKT2: amplification of AKT1 in a primary human gastric adenocarcinoma. Proc Natl Acad Sci U S A 1987;84:5034–7.
10. Wu G, Xing M, Mambo E, Huang X, Liu J, Guo Z, et al. Somatic mutation and gain of copy number of PIK3CA in human breast cancer. Breast Cancer Res 2005;7:R609–16.
11. Carpten JD, Faber AL, Horn C, Donoho GP, Briggs SL, Robbins CM, et al. A transforming mutation in the pleckstrin homology domain of AKT1 in cancer. Nature 2007;448:439–44.
12. Parikh C, Janakiraman V, Wu WI, Foo CK, Kljavin NM, Chaudhuri S, et al. Disruption of PH-kinase domain interactions leads to oncogenic activation of AKT in human cancers. Proc Natl Acad Sci U S A 2012;109:19368–73.
13. Lindhurst MJ, Sapp JC, Teer JK, Johnston JJ, Finn EM, Peters K, et al. A mosaic activating mutation in AKT1 associated with the Proteus syndrome. N Engl J Med 2011;365:611–9.
14. Brugge J, Hung MC, Mills GB. A new mutational AKTivation in the PI3K pathway. Cancer Cell 2007;12:104–7.
15. Clark AS, West K, Streicher S, Dennis PA. Constitutive and inducible Akt activity promotes resistance to chemotherapy, trastuzumab, or tamoxifen in breast cancer cells. Mol Cancer Ther 2002;1:707–17.
16. Schultze SM, Jensen J, Hemmings BA, Tschopp O, Niessen M. Promiscuous affairs of PKB/AKT isoforms in metabolism. Arch Physiol Biochem 2011;117:70–7.
17. Mattmann ME, Stoops SL, Lindsley CW. Inhibition of Akt with small molecules and biologics: historical perspective and current status of the patent landscape. Expert Opin Ther Patents 2011;21:1309–38.
18. Degtyarev M, De Maziere A, Orr C, Lin J, Lee BB, Tien JY, et al. Akt inhibition promotes autophagy and sensitizes PTEN-null tumors to lysosomotropic agents. J Cell Biol 2008;183:101–16.
19. Pal SK, Reckamp K, Yu H, Figlin RA. Akt inhibitors in clinical development for the treatment of cancer. Expert Opin Investig Drugs 2010;19:1355–66.
20. Davies BR, Greenwood H, Dudley P, Crafter C, Yu DH, Zhang J, et al. Preclinical pharmacology of AZD5363, an inhibitor of AKT: pharmacodynamics, antitumor activity, and correlation of monotherapy activity with genetic background. Mol Cancer Ther 2012;11:873–87.
21. Rhodes N, Heerding DA, Duckett DR, Eberwein DJ, Knick VB, Lansing TJ, et al. Characterization of an Akt kinase inhibitor with potent pharmacodynamic and antitumor activity. Cancer Res 2008;68:2366–74.
22. Wallin JJ, Guan J, Wei Prior W, Lee LB, Berry L, Belmont LD, et al. GDC-0941, a novel class I selective PI3K inhibitor, enhances the efficacy of docetaxel in human breast cancer models by increasing cell death *in vitro* and *in vivo*. Clin Cancer Res 2012;18:3901–11.
23. Vitolo MI, Weiss MB, Szmacinski M, Tahir K, Waldman T, Park BH, et al. Deletion of PTEN promotes tumorigenic signaling, resistance to anoikis, and altered response to chemotherapeutic agents in human mammary epithelial cells. Cancer Res 2009;69:8275–83.
24. Corey E, Quinn JE, Buhler KR, Nelson PS, Macoska JA, True LD, et al. LuCaP 35: a new model of prostate cancer progression to androgen independence. Prostate 2003;55:239–46.
25. Wallin JJ, Edgar KA, Guan J, Berry M, Prior WW, Lee L, et al. GDC-0980 is a novel class I PI3K/mTOR kinase inhibitor with robust activity in cancer models driven by the PI3K pathway. Mol Cancer Ther 2011;10:2426–36.
26. Blake JF, Xu R, Bencsik JR, Xiao D, Kallan NC, Schlachter S, et al. Discovery and preclinical pharmacology of a selective ATP-competitive Akt inhibitor (GDC-0068) for the treatment of human tumors. J Med Chem 2012;55:8110–27.
27. Han EK, Leverson JD, McGonigal T, Shah OJ, Woods KW, Hunter T, et al. Akt inhibitor A-443654 induces rapid Akt Ser-473 phosphorylation independent of mTORC1 inhibition. Oncogene 2007;26:5655–61.
28. Okuzumi T, Fiedler D, Zhang C, Gray DC, Aizenstein B, Hoffman R, et al. Inhibitor hijacking of Akt activation. Nat Chem Biol 2009;5:484–93.

Published OnlineFirst January 3, 2013; DOI: 10.1158/1078-0432.CCR-12-3072

29. Lin K, Lin J, Wu WI, Ballard J, Lee BB, Gloor SL, et al. An ATP-site on-off switch that restricts phosphatase accessibility of Akt. Sci Signal 2012; 5:ra37.
30. Hoeflich KP, O'Brien C, Boyd Z, Cavet G, Guerrero S, Jung K, et al. *In vivo* antitumor activity of MEK and phosphatidylinositol 3-kinase inhibitors in basal-like breast cancer models. Clin Cancer Res 2009;15:4649–64.
31. Vasudevan KM, Barbie DA, Davies MA, Rabinovsky R, McNear CJ, Kim JJ, et al. AKT-independent signaling downstream of oncogenic PIK3CA mutations in human cancer. Cancer Cell 2009;16: 21–32.
32. Dan S, Okamura M, Seki M, Yamazaki K, Sugita H, Okui M, et al. Correlating phosphatidylinositol 3-kinase inhibitor efficacy with signaling pathway status: *in silico* and biological evaluations. Cancer Res 2010;70:4982–94.
33. O'Brien C, Wallin JJ, Sampath D, GuhaThakurta D, Savage H, Punnoose EA, et al. Predictive biomarkers of sensitivity to the phosphatidylinositol 3′ kinase inhibitor GDC-0941 in breast cancer preclinical models. Clin Cancer Res 2010;16:3670–83.
34. Chou TC, Talalay P. Inhibition of ATP: L-methionine S-adenosyltransferase of bakers' yeast by structural analogues of ATP. Biochim Biophys Acta 1973;321:467–74.
35. Tan SX, Ng Y, James DE. Akt inhibitors reduce glucose uptake independently of their effects on Akt. Biochem J 2010;432:191–7.
36. Burris HA, Siu LL, Infante JR, Wheler JJ, Kurkjian C, Opalinska J, et al. Safety, pharmacokinetics (PK), pharmacodynamics (PD), and clinical activity of the oral AKT inhibitor GSK2141795 (GSK795) in a phase I first-in-human study. J Clin Oncol 2011;29:suppl; abstr 3003.
37. Tabernero J, Saura C, Perez DR, Dienstmann R, Rosello S, Prudkin L, et al. First-in-human phase I study evaluating the safety, pharmacokinetics (PK), and intratumor pharmacodynamics (PD) of the novel, oral, ATP-competitive Akt inhibitor GDC-0068. J Clin Oncol 29:2011 (suppl; abstr 3003).
38. Yap TA, Yan L, Patnaik A, Fearen I, Olmos D, Papadopoulos K, et al. First-in-man clinical trial of the oral pan-AKT inhibitor MK-2206 in patients with advanced solid tumors. J Clin Oncol 2011;29: 4688–95.